Implicit-Explicit Method for Solving the Navier-Stokes Equations

J. S. Shang*
Air Force Flight Dynamics Lab., Wright-Patterson Air Force Base, Ohio

An implicit-explicit numerical method has been developed for obtaining asymptotic steady-state solutions of the Navier-Stokes equations. The numerical solution of practical engineering problems requires fine spatial mesh distributions to resolve viscous layers near wall boundaries. The fine mesh, coupled with the stability limitations of fully explicit methods, yields large computing times. The implicit-explicit algorithm has been developed for obtaining solutions to the Navier-Stokes equations to reduce the computational time required. The implicit method is used in regions where the fine mesh is required, while the explicit method is retained in the remainder of the flowfield. Numerical solutions are obtained for two- and three-dimensional strong inviscid-viscous interactions. The present method exhibits an order of magnitude reduction in computing time over the fully explicit method with comparable accuracy.

Nomenclature

A,B,C,D	= coefficients of the linearized equation [Eq. (11)] for the implicit operator in η
A',B',C',D'	= coefficients of the linearized equation [Eq. (12)] for the implicit operator in ζ
e	= internal energy, $c_v T + (u^2+v^2+w^2)/2$
F,G,H	= flux vectors, Eq. (4)
i,j,k	= index for grid point
L_ξ, L_η, L_ζ	= difference operators
P	= static pressure
$\dot{q}$	= heat flux, $-k \nabla T$
t	= time
T	= static temperature
$\bar{u}$	= velocity components in Cartesian frame (u,v,w)
$\bar{U}$	= dependent variables
x,y,z	= Cartesian coordinates
ξ,η,ζ	= transformed coordinates, Eq. (5)
k	= molecular heat conductivity
ρ	= density
$\bar{\bar{\tau}}$	= stress tensor
$\|\ \|$	= root-mean-square values

Subscripts

imp	= implicit procedure
exp	= explicit procedure
∞	= properties evaluated at the freestream condition

Superscripts

n	= time level $n\,\Delta t$
$*$	= time level $(n+\frac{1}{2})\,\Delta t$
$**$	= time level $(n+1)\,\Delta t$

I. Introduction

A SIGNIFICANT number of numerical solutions of the compressible Navier-Stokes equations have been obtained utilizing MacCormack's explicit finite difference method.[1-4] Due to the small time step limitation dictated by stability requirements of this method, excessive computing times are required to solve high Reynolds number problems. It is logical then to explore numerical methods which would relieve the severity of this limitation.[5-7]

Since the fully explicit method[1,2] is conditionally stable, the stability condition (CFL) severely limits the allowable time step. For the diffusion-dominated flow region, MacCormack and Baldwin[2] have shown that the time step satisfying the stability condition is proportional to the square of the mesh spacing aligned with the factorized operator. However, this restriction can be removed by incorporating an implicit procedure which possesses a more favorable stability property, permitting a much larger time step to be used. In general, for aerodynamic problems a fine mesh spacing is required only in the direction normal to the solid contour. Therefore, this implicit scheme only needs to be implemented in the direction normal to the surface and confined to the domain immediately adjacent to the solid surface.

MacCormack[8,9] demonstrated that by a combination of an implicit-explicit scheme and further equation splitting, an order of magnitude gain in computational efficiency over his early explicit method[1,2] was possible. The equation-splitting concept was introduced by Ames[10] and is conceptually similar to the fractional step methods (time splitting).[3,11] The basis of the equation-splitting idea is to group widely varying eigenvalue functions and solve the split equations individually. For the Navier-Stokes equations, the system of equations is first reduced to several one-dimensional equations by time splitting, with the portion containing the inviscid terms solved first and then the portion containing the dissipative terms.[8,9,12] The equation-splitting method is heuristic,[10] but has been successfully demonstrated by both MacCormack and Dodge.[12]

The basic idea of the present analysis may be considered as a modification to MacCormack's rapid implicit-explicit scheme, in which an implicit-explicit scheme is adopted for the time-split equations in regions according to the flowfield characteristics and the equation-splitting technique is eliminated. The present analysis is also conceptually similar to the recent work by Li,[13] but was independently developed. For the present analysis, the implicit procedure is used to solve the time-split equations in the directions normal and adjacent to the surface, while the rest of the flowfield is still evaluated by the explicit scheme.[1,2,7] The minimum time step in the fine mesh region is no longer bounded by the stability condition which requires $(\Delta t)_{\max} \le P_r \rho\ \Delta y^2/2\gamma\mu^6$. In the outer region where the explicit scheme is used, the relatively large Δy becomes comparable to the Δx step, resulting in

Presented as Paper 77-646 at the AIAA 3rd Computational Fluid Dynamics Conference, Albuquerque, N. Mex., June 27-28. 1977; submitted July 15, 1977; revision received Nov. 17, 1977.

Index categories: Computational Methods; Jets, Wakes, and Viscid-Inviscid Flow Interactions.

*Aerospace Engineer. Member AIAA.

much larger allowable time steps. Since a successful explicit procedure existed,[7] hopefully minor modifications of the explicit code would result in an order of magnitude improvement in computing time.

In the application of MacCormack's rapid solving method to multidimensional arbitrary geometrical configurations, a series of polyhedrons or polygons is constructed to define individual control volumes.[8,9] An alternative approach is to introduce a general coordinate transformation to describe arbitrary configurations.[7] The two approaches are equivalent through Stokes' theorem. The coordinate transformation also permits the implicit method to be used for the difference operator in the direction normal to the solid contour. Although the entire gain in efficiency achieved by MacCormack may not be obtained, simplification of the numerical coding was achieved.

The purpose of this paper is to evaluate the anticipated gain in computational efficiency by a generalized implicit-explicit solving scheme, and to assess the accuracy of the method by comparison with previous numerical results and experimental data.[14,15] The selected problems to be solved are: a two-dimensional supersonic shock wave/boundary-layer interaction and a three-dimensional hypersonic compression corner problem. Both problems contain separated flows due to strong inviscid-viscous interactions and have been reported in the literature.[14,15]

II. Analysis

A. Governing Equations and Solving Scheme

The governing equations of the present analysis are the three-dimensional, unsteady Navier-Stokes equations. In the absence of external forces, the conservation equations are presented as follows:

$$\frac{\partial \rho}{\partial t} + \nabla \cdot (\rho \bar{u}) = 0 \tag{1}$$

$$\frac{\partial \rho \bar{u}}{\partial t} + \nabla \cdot (\rho \bar{u}\bar{u} - \bar{\bar{\tau}}) = 0 \tag{2}$$

$$\frac{\partial \rho e}{\partial t} + \nabla \cdot (\rho e \bar{u} - \bar{u} \cdot \bar{\bar{\tau}} + \bar{q}) = 0 \tag{3}$$

which are in perfect divergence form. The system of equations in terms of flux vectors yields

$$\frac{\partial \bar{U}}{\partial t} + \frac{\partial \bar{F}}{\partial x} + \frac{\partial \bar{G}}{\partial y} + \frac{\partial \bar{H}}{\partial z} = 0 \tag{4}$$

where the vectors are defined in Ref. 7. Introducing a coordinate system transformation with sufficient flexibility to accommodate a large category of aerodynamic configurations as

$$\xi = \xi(x) \qquad \eta = \eta(x,y,z) \qquad \zeta = \zeta(x,y,z) \tag{5}$$

we have

$$\frac{\partial \bar{U}}{\partial t} + \xi_x \frac{\partial \bar{F}}{\partial \xi} + \sum_i \eta_{x_i} \frac{\partial \bar{G}_i}{\partial \eta} + \sum_i \zeta_{x_i} \frac{\partial \bar{H}_i}{\partial \zeta} = 0$$

$$i = 1,2,3; \quad x_1 = x, \quad x_2 = y, \quad x_3 = z \tag{6}$$

where ξ_x, η_{xi}, and ζ_{xi} are the partial derivatives of the transformed coordinates with respect to the Cartesian frame. If the Jacobian does not vanish at any point of the investigated domain, the transformation is admissible.[16] The dependent variables $\bar{U}(\rho, \rho\bar{u}, \rho e)$ are not altered.

The equation is time-split as follows:[3,11,17-19]

$$\bar{U}^{n+2} = L_\zeta(\Delta t/2) L_\eta(\Delta t/2) L_\xi(\Delta t) L_\eta(\Delta t/2) L_\zeta(\Delta t/2) \bar{U}^n \tag{7}$$

L_ξ, L_η, and L_ζ are the difference operators aligned with ξ, η, and ζ coordinates, respectively. It can be shown that the solution is second-order accurate in time and space, if each factorized operator is second-order accurate and the difference operators of the mixed derivative are commutative.[3]

The operators may be subdivided further into those portions solved by either implicit or explicit means. The implicit method is used for a portion of the domain in the fine grid region near the wall, while the remainder is evaluated by an explicit procedure.

Only L_η and L_ζ are affected, since L_ξ is selected to be in the direction of small gradients.

$$L_\eta(\Delta t/2) = L_{\eta_{\text{imp}}}(\Delta t/2), L_{\eta_{\text{exp}}}(\Delta t/2) \tag{8}$$

$$L_\xi(\Delta t/2) = L_{\zeta_{\text{imp}}}(\Delta t/2), L_{\zeta_{\text{exp}}}(\Delta t/2) \tag{9}$$

The difference operators L_η and L_ζ consist of implicit and explicit procedures for different domains. The matching points JFM and KFM are the common nodes between the implicit and explicit computations for L_η and L_ζ, respectively. The explicit differencing operators $L_\xi, L_{\eta\text{exp}}$, and $L_{\zeta\text{exp}}$ retain the conventional MacCormack explicit form.[1,2] The scheme is a two-step noncentered method. However, at the completion of the predictor-corrector operation, the method approaches a central-difference approximation.

In the present investigation, the splitting of the implicit and explicit operators is given as

$$\begin{aligned}\bar{U}^{n+2} = {} & [L_{\zeta_{\text{imp}}}(\Delta t/2), L_{\zeta_{\text{exp}}}(\Delta t/2)] \\ & [L_{\eta_{\text{imp}}}(\Delta t/2), L_{\eta_{\text{exp}}}(\Delta t/2)]\, L_{\xi_{\text{exp}}}(\Delta t) \\ & [L_{\eta_{\text{exp}}}(\Delta t/2), L_{\eta_{\text{imp}}}(\Delta t/2)] \\ & [L_{\zeta_{\text{exp}}}(\Delta t/2), L_{\zeta_{\text{imp}}}(\Delta t/2)]\, \bar{U}^n\end{aligned} \tag{10}$$

The maximum allowable time-step increment $(\Delta t)_{\max}$ in the present scheme is still limited by the stability condition (CFL) of the explicit operator, and usually it is of the same order of magnitude as the $L_{\xi\text{exp}}$ operators.

B. Implicit Operator and Matching Condition

The implicit operator is intended only to be used in the diffusion-dominated region where the coalescing compression waves are expected to have limited strength. Therefore, the need to express the variables in conservation form may not be required. In the present analysis, the primitive variables ρ, $\bar{u}$, T are adopted for simplicity in the implicit procedure. In order to make the implicit and explicit operators compatible, the implicit method was established as a two time-level (backward in time) and central space approximation. In addition, a Crank-Nicolson scheme was also incorporated as an option for comparison purposes. The fractional time-level operation permits a straightforward linearization of the governing equations without overly compromising the favorable stability property.[20-22] However, in order to improve the convergence characteristics, a Newton-Raphson or quasilinearization approach is used.[5] The viscous dissipation functions and mixed derivatives are evaluated explicitly, lagged by a fractional time step. The final system of equations in the η direction are given as

$$\frac{\partial \bar{U}_L}{\partial t} + \sum_L A_L \frac{\partial^2 \bar{U}_L}{\partial \eta^2} + \sum_L B_L \frac{\partial \bar{U}_L}{\partial \eta} + \sum_L C_L \bar{U}_L + D_L = 0 \quad L = 1,2,\ldots 5 \tag{11}$$

Similarly for the ζ direction, we have

$$\frac{\partial \bar{U}_L}{\partial t} + \sum_L A'_L \frac{\partial^2 \bar{U}_L}{\partial \zeta^2} + \sum_L B'_L \frac{\partial \bar{U}_L}{\partial \zeta} + \sum_L C'_L \bar{U}_L + D'_L = 0 \quad L = 1,2,\ldots 5 \tag{12}$$

where the dependent variable $\bar{U}$ is defined to be $\bar{U}(\rho,u,v,w,T)$. The preceding system contains five scalar equations for continuity, momentum, and energy. In principle, the system of five equations can be coupled and solved simultaneously, but the required arithmatic operations would be $(3N\text{-}2)\ (L^3+L^2)$ or $450N\text{-}300$ for a single row of points.[21,23] On the other hand, a system of equations organized as three coupled equations and two single tridiagonal systems for a single row of points, requires only $118N\text{-}80$ arithmetic operations. The advantage of the later cascading procedure in computational efficiency is significant, provided both methods have similar convergence properties. An appropriate sequence order is also critical, in that the ordering of the solving sequence must be such that the most dominant dependent variables in the sweep direction are coupled. The directional bias provides an obvious selection criterion. In the present analysis, for the sweep in the η direction, the variables ρ,v,T are solved, coupled, and followed by u and w individually. For the sweep in the ζ direction, variables ρ,w,T are found by solving the coupled equations, and then u and v are found.

As an example, the system of equations are given for the first fractional time step.

$$\frac{\partial \bar{U}_L^*}{\partial t} + \sum_1^3 A_L \frac{\partial^2 \bar{U}_L^*}{\partial \eta^2} + \sum_1^3 B_L \frac{\partial \bar{U}_L^*}{\partial \eta} + \sum_1^3 C_L \bar{U}_L^* = -\sum_4^5 A_L \frac{\partial^2 \bar{U}_L^n}{\partial \eta^2} - \sum_4^5 B_L \frac{\partial \bar{U}_L^n}{\partial \eta} - \sum_4^5 C_L \bar{U}_L^n - D_L \tag{13}$$

$$\frac{\partial \bar{U}_4^*}{\partial t} + A_4 \frac{\partial^2 \bar{U}_4^*}{\partial \eta^2} + B_4 \frac{\partial \bar{U}_4^*}{\partial \eta} + C_4 \bar{U}_4^* = -\sum_1^5 A_L \frac{\partial^2 \bar{U}_L^n}{\partial \eta^2} - \sum_1^5 B_L \frac{\partial \bar{U}_L^n}{\partial \eta} - \sum_1^5 C_L \bar{U}_L^n - D_4 \quad L \neq 4 \tag{14}$$

$$\frac{\partial \bar{U}_5^*}{\partial t} + A_5 \frac{\partial^2 \bar{U}_5^*}{\partial \eta^2} + B_5 \frac{\partial \bar{U}_5^*}{\partial \eta} + C_5 \bar{U}_5^* = -\sum_1^4 A_L \frac{\partial^2 \bar{U}_L^n}{\partial \eta^2} - \sum_1^4 B_L \frac{\partial \bar{U}_L^n}{\partial \eta} - \sum C_L \bar{U}_L^n - D_5 \tag{15}$$

where $\bar{U}_1=\rho$, $\bar{U}_2=v$, $\bar{U}_3=T$, $\bar{U}_4=u$ and $\bar{U}_5=w$. The superscript * indicates the dependent variables evaluated at time level $(n+\frac{1}{2})\,\Delta t$, where the superscript n designates the dependent variable at time level $t=n\Delta t$.

The Crank-Nicolson scheme is a second-order accurate method in time and spatial variables. On the other hand, the implicit scheme is second-order accurate in spatial variables only. In order to improve the accuracy in time for the implicit scheme, an approach analogous to the ADI technique could be used. However, in the present analysis, the second fractional time-step calculation was simply the repetitive operation of the first, after updating all the coefficients (A,B,C,D) to $\Delta t(n+\frac{1}{2})$, * level. The dependent variables $\bar{U}$ then were evaluated at the final time level **, $(n+1)\,\Delta t$. The time-averaged procedure

$$\bar{U}^{n+1} = \bar{U}^n + \left(\frac{\partial U^*}{\partial t} + \frac{\partial U^{**}}{\partial t}\right)\Big/ 2$$

was also used to give an identical formal temporal accuracy to that of the explicit operators. No iteration process was used for each time step. The coupled system of equations was solved by using a Gaussian elimination scheme with row pivoting for solving a set of band equations.[24] The uncoupled equations were evaluated by the Thomas algorithm.[5,19,23]

Since the present method switches numerical schemes from an implicit to an explicit numerical algorithm across the matching point, particular caution must be exercised to ensure strict conservation and local consistency[25,26] at this point. The matching procedure is also uniquely determined by the two schemes it connects. This matching condition is satisfied by imposing a Dirichlet type of boundary condition for the implicit calculation at the matching point (JFM or KFM), and performing the explicit calculation including the matching point. MacCormack's explicit scheme ensures conservation of vector flux at the matching point. Although difficulty was anticipated at the matching point, no wiggles or discernable errors were observed with the procedure employed as just described.

C. Initial and Boundary Conditions

The boundary conditions vary widely between the two investigated inviscid-viscous interacting problems. However, a general description can be given.

The initial condition is

$$\bar{U}(0,\xi,\eta,\zeta) = \bar{U}_\infty \tag{16}$$

The far field is straightforward; for the three-dimensional problem, the no-change condition[7] is imposed to insure a two-dimensional asymptotic behavior away from the corner. For the two-dimensional shock wave/boundary-layer interaction, the incident oblique shock intercepts the boundary of the computational domain, thus the Rankine-Hugoniot conditions are used downstream of the shock intersection.

The upstream condition satisfies the unperturbed freestream condition and is designed to be located a single step away from the leading edges.

$$\bar{U}(t,\xi_i,\eta,\zeta) = \bar{U}_\infty \tag{17}$$

The far-downstream condition requires gradients of flow properties to vanish $(\partial U/\partial \xi = 0)$.[1,2,7-9]

The boundary conditions at the surface consist of the no-slip condition for the velocity components and either a constant surface temperature or adiabatic wall condition, depending on the accompanying experimental condition.[14,15] The density (or pressure) condition at the surface is the satisfaction of a compatibility relationship derived from the normal momentum equation, which reduces to a simple zero pressure gradient approximation at the surface for most engineering problems.[7]

Discussion of Results

All the numerical calculations were performed on a CDC 6600 digital computer. The presentation of the results includes the general features of the implicit-explicit numerical method, characteristics of the temporal convergence, spatial truncation error analysis and specific comparisons with known numerical results, and experimental measurements for the two-dimensional case. The numerical results for the three-dimensional corner configuration are also given.

Two-Dimensional Results

In Table 1, the general features of the fully explicit and the implicit-explicit hybrid procedure are given for the two-dimensional shock impingement problem. The hybrid procedure includes both the simple implicit and the Crank-Nicolson method. All the calculations were performed for a 28×22 grid point distribution. The minimum and the

Table 1 Two-dimensional shock impingement problem

	Explicit	Implicit-Explicit	
		Crank-Nicolson	Implicit
$(\Delta t)_{max}/\Delta t_{CFL}$	1.0	12.5	25
Computing time, t_c, min.	90.0	15.1	10.4
$t_c/t_{c_{imp}}$	8.62	1.44	1.0
Matching point, JFM		10	12

maximum Δy were 0.9955×10^{-4} ft and 0.1741×10^{-1} ft, respectively, and were stretched geometrically. However, in the transformation plane, the step size in $\Delta\eta$ was uniform. Since no coordinate transformation was incorporated for x, Δx was identical to $\Delta\xi$ with a value of 0.11083×10^{-1} ft. The solution was allowed to evolve with time until the accumulated time step reached seven times the value of the characteristic time scale t_{ch}. The characteristic time was defined as the time required for a fluid particle to travel over the characteristic length ($L=0.1625$ ft) at freestream speed ($t_{ch}=9.68\times10^{-5}$ s).

An error analysis of the central differencing formulation yielded a leading term truncation error in the viscous region $\|U_{\eta\eta\eta}\ \Delta\eta^2/3!\ U_{\eta}\|$ to be 4%. The second-order derivative approximation $\|2U_{\eta\eta\eta\eta}\ \Delta\eta^2/4!\ U_{\eta\eta}\|$ was around 0.25%. The truncation errors for derivatives in the ξ direction were lower by a factor of three or more. The maximum difference between the three calculations was found in predicting C_f near the reattachment point; the discrepancy being about 7%. The Crank-Nicolson scheme indicated an erratic behavior for time step size greater than 12.5 Δt_{CFL} and failed to converge. This particular behavior had been previously reported.[8,9,13,19]

From Table 1, it is obvious that the implicit-explicit hybrid scheme provides a significant gain in computing efficiency without degrading accuracy. For turbulent flow, a substantial refinement of the grid near the wall is required to resolve the laminar sublayer. Therefore, the present scheme is expected to increase the calculation speed several orders of magnitude over that of an explicit procedure. For the two-dimensional problem investigated, the present scheme has a factor of 8.62 gain over the fully explicit scheme. This improvement is comparable to the 6.4 factor realized by MacCormack's implicit-explicit scheme.[8,9]

In Fig. 1, the characteristics of the iterative convergence of the present method is presented for the calculations with a 28×33 grid. Both the simple implicit and the Crank-Nicolson method are given. Again the skin friction coefficient was found to be the slowest parameter to converge. The reflected shock pressure reached its asymptote at about 2 t_{ch}. The conventional relative error criterion $\Sigma_i\Sigma_j[(\Delta\bar{U}/\bar{U}_\infty)^2]^{1/2}/(i\cdot j)$ was found to be inadequate, because it remained nearly constant ($\sim10^{-4}$) after 2 t_{ch} while the value of C_f continued to evolve slowly. The two most representative skin friction coefficients at $\bar{x}=0.300$ and $\bar{x}=0.966$ were monitored. After 5 t_{ch} in time the value of C_f upstream reached its asymptote, but the value of C_f downstream of the separation zone continued its evolution at a rate of -0.76% per characteristic time. The solution by the Crank-Nicolson scheme exhibited identical behavior, and the Crank-Nicolson scheme is known to be second-order accurate in time.[19] In all, the trend of convergence is orderly and monotonically approaches the steady-state asymptotes at different rates, depending on the relative location from the leading edge.

The existence of a rapid computing procedure made practical the investigation of an error analysis by comparing several different grid sizes. In Fig. 2, the result of a truncation error analysis is presented. Comparison of two computations of 28×33 and 42×33 grid systems showed no distinguishable difference in values of C_f. A sample analysis of leading truncated terms for the first- and second-order derivative also revealed that the error in the η direction was greater than in the ξ direction by a factor of 4. A truncation error analysis in the η direction was performed by comparing the numerical results with three different grid point distributions: 28×22, 28×33, and 28×44. The numerical results by the finest mesh point distribution was also compared with Richardson extrapolations[19] for the second-order methods. Several values of C_f presented in Fig. 2 indicate that the present scheme is indeed a second-order accurate method in spatial variables.

The surface pressure distribution for the calculation with the 28×33 grid point distribution together with MacCormack's result[8,9] with a 32×32 grid and experimental data[14] is presented in Fig. 3. The maximum difference between MacCormack's result and the present one is less than 2%. The computing time for this calculation was 16.90 min for the implicit scheme. The Crank-Nicolson method, on the other hand, required 24.61 min to reach six characteristic time steps, t_{ch}.

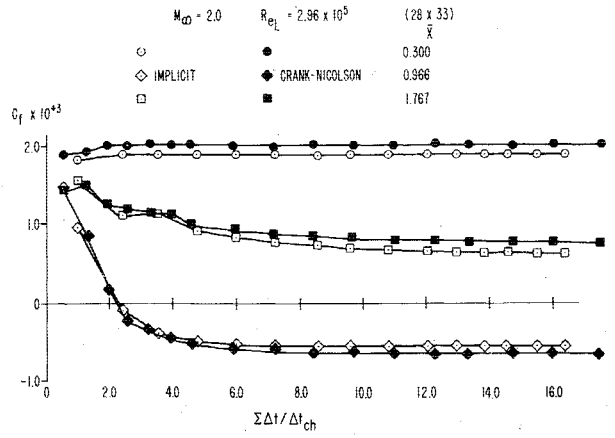

Fig. 1 Time-convergence characteristics.

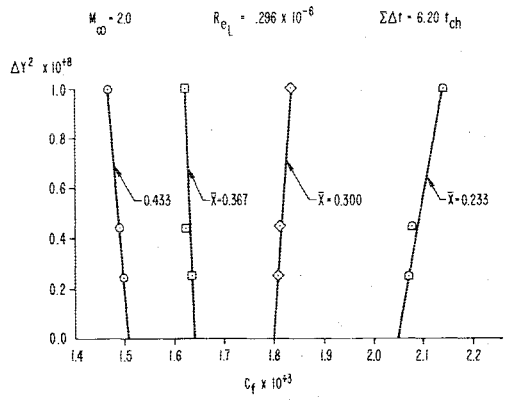

Fig. 2 Truncation error representation.

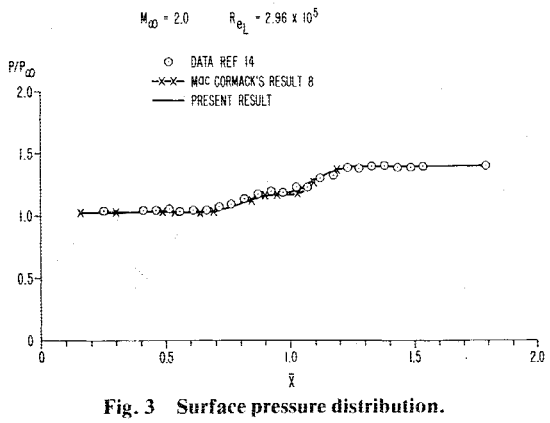

Fig. 3 Surface pressure distribution.

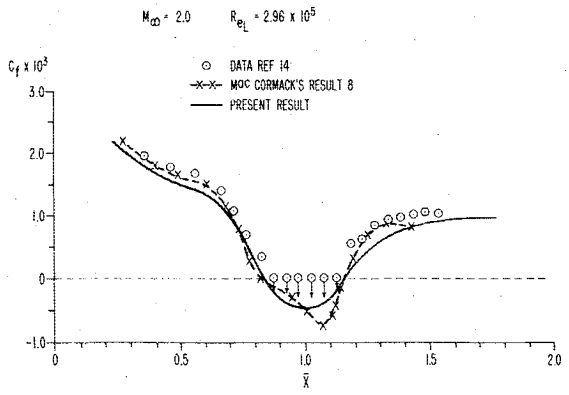

Fig. 4 Skin friction coefficient distribution.

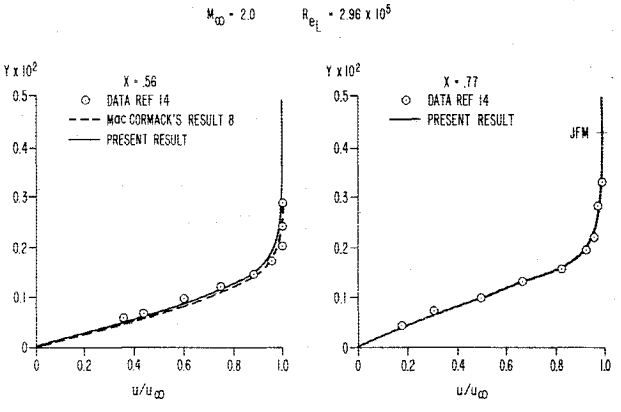

Fig. 5 Comparison of velocity profiles.

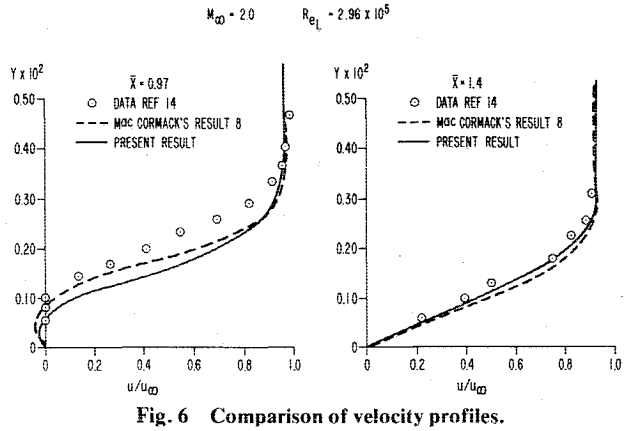

Fig. 6 Comparison of velocity profiles.

In Fig. 4, the skin friction coefficient distributions of MacCormack's results, experimental data, and the present calculation (implicit) are presented. The length of separation is predicted within 3% between calculations. However, there is a behavioral difference within the region of flow separation; MacCormack's result exhibits a near "dual-minimum" distribution. This particular trend is known to be associated with the definition of the pressure plateau in the separation region.[27] The difference in Fig. 3 has been mentioned previously and will be delineated in discussing the next two figures. The maximum difference between the calculations of the Crank-Nicolson method and the implicit scheme is less than 3%.

The detailed flowfield structure is presented in Fig. 5 and 6 in terms of velocity profiles at several selected streamwise locations with accompanying data. MacCormack's results are also included where available. The difference between the present results for the velocity profiles is negligible, therefore

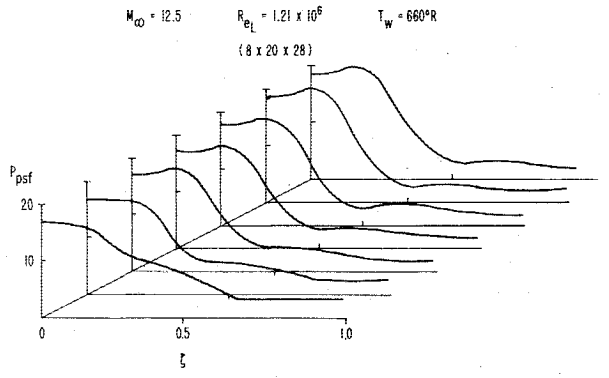

Fig. 7 Plate surface pressure distribution for a three-dimensional corner.

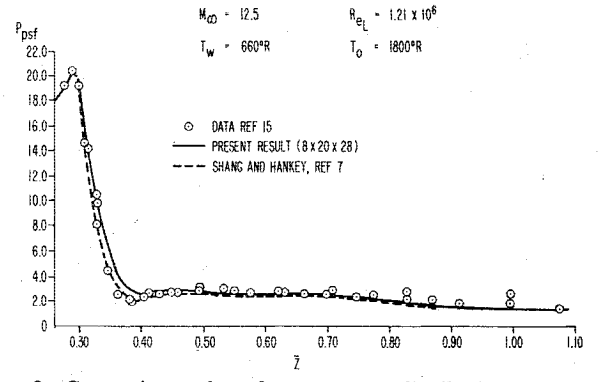

Fig. 8 Comparison of surface pressure distribution in conical coordinates.

only the implicit calculations will be given. Excellent agreement is indicated between experimental measurement[14] and numerical results, except perhaps in the reverse flow region. At $\Delta x = 0.97$, both MacCormack's result and the present calculation underpredict the experiment in the reverse flow region, with the present result exhibiting a greater discrepancy in comparison with data. The observed deficiency can be attributed to the inferior numerical resolution due to the variable step sizes. The present scheme clusters grid points near the plate by a geometric variation; the first point away from the surface has a step size Δy of 0.6751×10^{-4} ft; at the matching point (JFM = 16), $Y = 0.428 \times 10^{-2}$ ft the step size, Δy has been stretched to a value of 0.727×10^{-3}. MacCormack, on the other hand, used a uniform fine mesh ($\Delta y = 0.50 \times 10^{-3}$ ft) for the viscous-dominated region. The difference may reflect the conservation error[19,22,25,26] due to the use of primitive variables in this viscous domain. However, similar difference was also observed between MacCormack's result and that of Beam and Warming,[6] even though both employed the conservative formulation. In principle, this discrepancy can be removed by further reducing the grid spacing. The calculation using the finest mesh distribution (28×44) shows substantial improvement in comparison with the experimental measurement, but should not be considered a fair comparison with MacCormack's result for the 32×32 mesh system.

Three-Dimensional Results

The detailed geometrical configuration, the coordinate transformation, and the mesh point system of the three-dimensional corner problem can be found in Ref. 7. In essence, the flowfield in the corner region by a 15 deg wedge and a flat plate was investigated at a Mach number of 12.5 and a characteristic Reynolds number of 1.21×10^6. In the present analysis, the three-dimensional corner problem is evaluated by the implicit-explicit hybrid scheme for a grid

point distribution of $8\times20\times28$. In the transformed space, uniform step sizes for the three-dimensional problem are $\Delta\xi=0.1276$, $\Delta\eta=0.05263$, and $\Delta\zeta=0.03704$. However, in the physical space the range of y and z are stretched linearly in a conical coordinate system. At each constant x plane the step sizes in y and z, Δy, Δz are further clustered in geometrical proportion. The minimum Δy and Δz are required to be $L/2(R_{eL})^{1/2}$ (0.4728×10^{-3}). The geometrical variation parameters assume the values of 2.154 (y) and 3.248 (z), respectively. The total central memory used was 260,500 words (base 8).

Since the original computation[7] was performed without the advantage of equation splitting for fractional time step, for each unit characteristic time step 292 min of computer time was required. A total elapsed time of five characteristic time steps ($t_{ch}=0.2185\times10^{-3}$ s) was accumulated to obtain the asymptotic steady-state solution. Preliminary results indicate that the implicit-explicit hybrid scheme required only 27.7 min to achieve one characteristic time step. The ratio of required computing times is 10. However, numerical oscillations have been observed in the solutions for relatively coarse grid point distributions. Higher order dissipation terms may be required to damp this short wavelength.[6] Effort is currently being undertaken to investigate this phenomenon. In order to avoid the repetitious presentations of the numerical results, only the surface pressure distribution for the entire flowfield and a specific comparison with known numerical result[7] and experimental measurement[14] are given.

In Fig. 7, the surface pressure distributions on the plate are given for the entire flowfield. To facilitate the visual identification, the pressure distributions are presented in the transformation variable ζ. The surface pressure reaches its peak value in the corner region across the wedge shock envelope. Moving outward, the surface pressure reveals an expansion zone.[7] The surface pressure eventually reaches the two-dimensional asymptote far away from the corner. The surface pressure also reveals the conical flow behavior which justifies the rather coarse step size in ξ.

In Fig. 8, the surface pressure distribution is presented and accompanied by the previously obtained explicit calculation[7] and experimental measurement.[14] The agreement between the measurements and numerical results is excellent. In general, the numerical results with the $8\times20\times28$ mesh system are confined within the data scattering. The maximum difference between numerical results is 10%.

Concluding Remarks

A three-dimensional, time-dependent, implicit-explicit hybrid numerical procedure for the Navier-Stokes equations has been developed. The numerical code also contains a general coordinate transformation capable of evaluating a wide range of aerodynamical configurations. This procedure is a second-order scheme in both space and time. Successful comparisons with an explicit method were performed for a supersonic, two-dimensional shock wave/boundary-layer interaction and a hypersonic three-dimensional compression corner flow at a high Reynolds number laminar flow condition.

Substantial gain in computing efficiency over conventional fully explicit methods[1,2,7] were realized, while retaining comparable accuracy. For the investigated two-dimensional problem, the present method reduces the computing time by a factor of 8.6. The numerical results in comparison with MacCormack's rapid solving scheme[8,9] exhibit a maximum difference of about 4%. However, MacCormack's equation splitting between inviscid and viscous terms is no longer required, and the approximation $v/c\ll1$ for his characteristic equation is also eliminated. For the three-dimensional problem, the gain in computing efficiency is reflected by a factor of ten increase in speed. The maximum difference in pressure between the fully explicit method and the present scheme is 10%. Unfortunately, time-dependent methods converge like $t^{-1/2}$ and, therefore, require excessive computer time to obtain higher precision. Improvements are needed to accelerate convergence.

Acknowledgment

The author is indebted to W. L. Hankey for his constant guidance and encouragement.

References

[1] MacCormack, R. W., "Numerical Solution of the Interaction of a Shock Wave with a Laminar Boundary Layer," *Lecture Notes in Physics*, Vol. 8, Springer-Verlag, N.Y., 1971, pp. 151-163.

[2] MacCormack, R. W. and Baldwin, B. S., "A Numerical Method for Solving the Navier-Stokes Equations with Application to Shock-Boundary Layer Interactions," AIAA Paper 75-1, Pasadena, Calif., Jan. 1975.

[3] Lomax, H., "Recent Progress in Numerical Techniques for Flow Simulation," *Proceedings of AIAA 2nd Computational Fluid Dynamics Conference*, Hartford, Conn., June 1975, pp. 1-9; also, *AIAA Journal*, Vol. 14, April 1976, pp. 512-518.

[4] Peyret, R. and Vivand, H., "Computation of Viscous Compressible Flows Based on the Navier-Stokes Equations," AGARDograph No. 212, Sept. 1975.

[5] Blottner, F. G., "Computational Techniques for Boundary Layers," AGARD-LS-73, *Computational Methods for Inviscid and Viscous Two- and Three-Dimensional Flow Fields*, Feb. 1975, pp. 3-1, and 3-51.

[6] Beam., R. M. and Warming, R. F., "An Implicit Factored Scheme for the Compressible Navier-Stokes Equations," Paper 77-654, Albuquerque, N. Mex., June 1977.

[7] Shang, J. S. and Hankey, W. L., "Numerical Solution of the Navier-Stokes Equations for a Three-Dimensional Corner," AIAA Paper 77-169, Los Angeles, Calif., Jan. 1977; also *AIAA Journal*, Vol. 15, Nov. 1977, pp. 1575-1582.

[8] MacCormack, R. W., "A Rapid Solver for Hyperbolic Systems of Equations," presented at the V International Computational Fluid Dynamics Meeting, Netherlands, June 1976.

[9] MacCormack, R. W., "An Efficient Numerical Method for Solving the Time-Dependent Compressible Navier-Stokes Equations at High Reynolds Number," NASA TMX-73-129, July 1976.

[10] Ames, W. F., Ed., *Nonlinear Partial Differential Equations*, Academic Press, N.Y., 1967, pp. 55-72.

[11] Yanenko, N. N., *The Method of Fractional Steps*, Springer-Verlag, Berlin, Germany, 1971.

[12] Dodge, P. R., "A Numerical Method for 2D and 3D Viscous Flows," AIAA Paper 76-425, San Diego, Calif., July 1976; also, *AIAA Journal*, Vol. 15, July 1977, pp. 961-965.

[13] Li, C. P., "A Numerical Study of Separated Flows Induced by Shockwave/Boundary-Layer Interaction," AIAA Paper 77-168, Los Angeles, Calif., Jan. 1977.

[14] Hakkinen, R. J., Greber, I., Trilling, I., and Abarbanel, S. S., "The Interaction of an Oblique Shock Wave with a Laminar Boundary Layer," NASA Memo 2-8-59W, 1959.

[15] Cooper, J. R. and Hankey, W. L., "Flow Field Measurements in an Asymmetric Axial Corner at $M=12.5$," *AIAA Journal*, Vol. 12, Oct. 1974, pp. 1353-1357.

[16] Sokolnikoff, J. S., ed., *Tensor Analysis Theory and Applications to Geometry and Mechanics of Continua*, 2nd ed., John Wiley & Sons, Inc., 1964, pp. 50-104.

[17] Douglas, J. and Gunn, J., "A General Formulation of Alternating Direction Methods," *Numerical Mathematics*, Vol. 6, No. 5, 1964.

[18] Richtmyer, R. D. and Morton, K. W., *Difference Methods for Initial-Value Problems*, 2nd ed., Interscience Publisher, 1967.

[19] Roache, P. J., *Computational Fluid Dynamics*, Hermosa Publishers, 1972.

[20] Briley, W. R., "Numerical Methods for Predicting Three-Dimensional Steady Viscous Flow in Ducts," *Journal of Computational Physics*, Vol. 14, Jan. 1974, pp. 8-28.

[21] McDonald, H. and Briley, W. R., "Three-Dimensional Supersonic Flow of a Viscous or Inviscid Gas," *Journal of Computational Physics*, Vol. 19, Oct. 1975, pp. 150-178.

[22] Levy, R., Shamroth, S. J., Gibeling, H. J., and McDonald, H., "A Study of the Turbulent Shockwave Boundary Layer Interaction," AFFDL-TR-76-163, Feb. 1977, Air Force Flight Dynamics Lab., Wright-Patterson AFB, Ohio.

[23] Isaacson, E. and Keller, H. B., *Analysis of Numerical Methods*, John Wiley & Sons, Inc., N.Y., 1966.

[24] Petty, J. S., "Research in Computational Fluid Dynamics (Final Report on Work Unit 09)," ARL TR 75-0209, Aerospace Research Labs., Wright-Patterson AFB, Ohio. Also private communication.
[25] Lax, P., "Weak Solutions of Nonlinear Hyperbolic Equations and their Numerical Computation," *Communications of Pure and Applied Mathematics*, Vol. 7, 1954, pp. 159-193.
[26] Warming, R. F. and Beam, R. M., "Upwind Second-Order Difference Schemes and Application in Aerodynamic Flows," *AIAA Journal*, Vol. 14, Sept. 1976, pp. 1241-1249.
[27] Shang, J. S., Hankey, W. L., and Law, C. H., "Numerical Simulation of Shock Wave-Turbulent Boundary-Layer Interactions," *AIAA Journal*, Vol. 14, Oct. 1976, pp. 1451-1457.